Available Online

International Journal of Advancements in Mathematics

ISSN: 2959-2755 (Print), 2959-2763 (Online)

http://www.scienceimpactpub.com/IJAM

Numerical Investigation of Active and Passive Control of MHD Oblique Stagnation Point Flow of Casson-Nano Fluid Along with Convective Boundary Conditions

Asifa Gul Bhatti[1†], **Malik Irfan**[1], **Kiran Pasha**[2]

Abstract In this paper, we are going to study the numerical investigation of oblique stagnation point flow of Casson-nano fluids along with convective boundary conditions. Mixed boundary conditions for active and passive control are also number, and presents the findings using tables and graphs. The study reveals that an increase in the Biot number and thermal radiation parameter results in an enhancement of the temperature distribution, while an increase in the suction/injection parameter causes a reduction in the velocity and temperature distributions for both injection and suction cases.

Keywords: Vertical sheet, Magnetohydrodynamics, Suction/Injunction, Casson fluid.

1. Introduction

The current study investigated the continuous stagnation factor in response to a Casson nano fluids movement in the corporation of convective boundary circumstances. The fluid travels in an Non-orthogonal motion along the height of the walls.

https://doi.org/10.52223/ijam.20222205

[†]Corresponding author: asifagul987@gmail.com

[1] School Education Department, Punjab, Pakistan

[2] Punjab Group of colleges, Quaidabad, Punjab, Pakistan.

Nanofluids have a variety of industrial uses, such electronic cooling systems, radiators, heat exchangers, super conductors, and beams of sunlight, and in the processing of industry. A nanoparticle is an infinitesimal molecule as a base one size aubstantially less than 100 nm. Nanoparticles studies is presently a place of excessive clinical hobby because of a huge kind of capacity programs in biomedical, optical and digital fields. Casson fluid is a non-Newtonian fluid that is well-known for its ability to produce stress. Ahmed et al. recently published a paper on kinematic flow that is time probably nanomaterials towards the point of standstill on a extended disk. They observed that the stretch layer parameter and incidence angle had an impact on the position of the static pressure. The analysis of heat transmission and the flow field is required to determine the end product's equality. The thermal radiation impact cannot be ignored in high-temperature technological processes. Ghaly and Elbarbary explored free convection heat transfer with the influence of radiation near the isothermal stretching sheet towards the stagnation point by Ghaly and Elbarbary (1).

Tamada studied two-dimensional stagnation point flows impinging sideways on a level plate that was wavering at a constant rate in 1979. Hiemenz has also used a similarity redesign to reduce Unsteady equations to non-linear ordinary differential equations in order to investigate two-dimensional stagnation drift. Stagnation point flow, as well as regular or indirect two-dimensional and axisymmetric flow, over the stretching sheet of this annoyance. Presently a days, the energy proficiency is a critical subject considering warm conductivity improvement among the investigators. The inclusion of nanofluids in the base fluid was considered by the investigators for this aim. Masuda et al. (1996) (2) first described liquid suspensions of microparticles or nanoparticles. Choi (3) then uses a word "nano - fluid" for the first time (1995). The concept of boundary layer flow plays a crucial role in fluid mechanics. In boundary layer flow thin layer of fluid is moving in contact to the solid surface and velocity is modified from zero to the free stream velocity. Boundary layer flow is divided into two types laminar flow and turbulent flow. Nanofluids are another modern form comprising a small number of particles of nanometer size (typically <100nm) of heat transfer fluid, that are suspended continuously, steadily in a fluid. A nanofluid is the study of liquid, called nanoparticles, containing nanometer sized particles. Metal, oxides, carbides or carbon nanotubes are regularly made up of nanoparticles used in nanofluids.

We investigated the non-orthogonal stagnation factor associated with Casson-nano fluid drift and convective boundary conditions flow. We'll create a system of partial differential equations that includes equations for continuity, momentum, and energy. Using appropriate similarity transformations, it is possible to investigate the presence of a solution in a system of nonlinear ordinary differential equations. The nonlinear ODEs. for momentum and energy are remodeled by adopting the similarity transformation in linear kind. Further, the skin friction coefficient, temperature and focus profiles are communicated in graph and talked about in detail. Heat switch of everyday stagnation waft on a stretching sheet changed into later discussed via way of means of Mahapatra and Gupta. (4) Non-Orthogonal and Two-dimensional stagnation many fluid mechanics applications, and also construction and real scientific inquiry, are interested in point flows putting stress on a flat wall. The goal of this paper is to discuss a Casson nanofluid's steady stagnation point flow, the governing non-linear partial differential equations of the hassle are provided after which transformed into non-linear normal differential equations with the aid of using the usage of comparable and non-comparable methods. We look at a numerical solution for Oblique Stagnation point flow over convective boundary conditions in this paper. For tolerable modification, the controlling flow and energy equations are transformed into ordinary differential equations using a similar manner. The following ordinary differential equations are numerically illuminated using the MATLAB tool. Graphs depict the effect of various flow parameters, suction parameters, stertching parameters, free stream parameters, and nanoparticles on the Skin friction Coefficient and streamlines. In industry and engineering, heating and movement conduction in the area of the static pressure on extending surfaces have practical uses, such as fan-assisted cooling of metallic plates, digital equipment, and nuclear reactors, food processing, and hot rolling, wire drawing, and etc. Aziz (5) investigated a similarity answer for a flat surface with a laminar thermal boundary layer and a convective surface boundary condition. Because of its usefulness in many practical applications, the study of stagnation point flows has received a lot of attention throughout the history of fluid dynamics. A solid wall can stifle flow in some cases, but a Stasis without charge point and row can exist inside the flowing region in some others. The hard or stretched sidewall takes up residence in whole perpendicular plane in a stagnation point, and the flowing sector is y>0. The fluid meets up with the

boundary in an orthogonal and obliquelar pattern. Many industrial operations depend on the movement of a fluid over a stretched plate. Extrusion adhesive tapes and coating layer applications onto rigid substrates are two examples. A mathematical model of the problem reliant on arrangement of differential conditions is worked by the calculation of issue, customary differential conditions followed from partial differential conditions are tackled utilizing shooting-technique. Graphically portrayals of speed, temperature and focus profiles are finished utilizing Matlab bvp4c codes. Every one of these profiles are investigated through administering actual boundaries. Because of its importance in many commercial and construction presentations, stagnation-point flows have remained popular in fluid mechanics. In many heat exchangers, these flows are critical. The chance of stagnation point flow was at first begun by Hiemen's (6). This idea also fastened by Howarth (7) and Homann (8) by Hiemen's discoveries. B.K Mahahtha et al. (Mahahtha, 2015) regarding a nanofluid's past a porous flow with gravity modulation, curvilinear transmission, and Kinematic warming, Pro. Eng. The thermal conductivity of non-metallic fluids is expected to be higher than that of metallic fluids so non-metallic fluids are excepted to have higher thermal conductivity.They proposed two methods to drive heat transfer ratio of nanofluid. These studies shows that the nanofluids have broad application prospects in industrial refrigeration, manufacturing, and biomedical applications explored by Bilal.M et al. (9). The two perpendicular as well as perpendicular pressure gradient streams having an impact on such a backwall are difficulties of keen importance in a variety of plasma physics procedures, such as in engineering fields. Aziz et al. (10) were explored loose convective boundary layer glide beyond a horizontal flat embedded in porous medium stuffed via way of means of nanofluid containing gyrotatic micro-organism. Buongiorno (11) has proposed two standard kinds of nanofluid numerical models. In different heat transfer applications, nanofluids are also thought about since the way forward for heat transfer fluid is. They expect nanoparticles to be framed by high warm conductivity leaving higher warm execution than certain life liquids. The goal of this research is to analyze the consequences of just a micropolar fluid magnetohydro flow of Porous medium having negligible typical fluxes of nanomaterials across an incrementally spreading plate in the presence of sunlight, convectively heated quantities, and then a viscous dissipation situation. Uddin et al. (Uddin, 2013) has expanded numerical results of slanted

stagnation point flow close by radiation impacts of non-newtonian nanofluids over an all inclusive surfaces. The convective boundary conditions in a MHD free convective micropolar fluid across a stertching piece of paper are the subject of this research. As a conventional fluids, Viscoelastic fluid will be used. Using proper transformations, development of appropriate differential equations are transformed into a set of boundary value problems. He analyzed impacts of all embeding parameters graphically for the temperature, concentration and flow fields. Numerical values of skin-friction coffi-cient, local Nusselt and Sherwood numbers for different parameters are calculated and analyzed. Recently Ellahi et al. (12; 13; 14) broke down the various issues for the most part centered around nonoparticle shape and other fluctuating properties of nanofluids. Active and passive are the two kinds of flow control methods which are utilized for accomplising an attractive change in the flow design and the boundary lawyer. Purusothaman et al. discovered that gravitational acceleration streams enclosed from an enclousre are still a primary component of heat capacity with natural circulation velocity distribution (Purusothaman 2017). Rajgopal et al. Rajgopal2015 have that Neither fluids a great interest in recent years because of their usefulness in industrial applications. He looked at the constant two different (angles) boundary layer flow of a nonlinear second-grade fluid approaching a stretching surface while incorporating temperature difference. When jets of unsteady flow infringe on a surface diagonally, he created oblique unsteady flow. Stagnation point flow looked at viscous dissipation circumstances by Lok et al.(15) this demonstrated as a specifying factor for the introduction of new control advancements. Currently being investigated fields due to its amazing applications, it has gained a lot of attention from researchers especially. Crane (16) (1970) investigated the nowadays there mixed convection flow and elastic deformation fluid caused by extending a flexible thin surface for its own dimension at a velocities that varied quadratic with length from a central object. Past a porous flow towards a stertching surface was explored by Mahapatra (2003) (17) and Sharma and Singh (2009) (18). They discovered that when the extending movement is smaller than the flow rate, a boundary layer forms. Labropulu et al. (19) examines the Non-orthogonal stagnation factor float in the direction of a bending plate with warmness exchange in a quasi fluid. These Casson fluid findings have demonstrated boundary layer flow over stretched surface faces in the absent of a titled magnetic force (20). In

1959, Casson proposed the model that was able to bear infinitely large viscosity without shear stress and conversely unlimited shear rate for zero viscosity. The detailed study of fluid flow along the stretched cylinder for the boundary layer was made by Ishak et al. (21; 22). Hsiao et al. (Hsiao, 2014) in the presence of Conductive heating and mechanical elastic forces at the static pressure, the as double flow and congugate heat flux of a quasi fluid were investigated. Ghaffari et al. (23) used parallel shooting methodologies to calculate various the non-orthogonal stagnation point flow over a stretching surface and reported that the obliqueness parmeter decreases the velocities. The coefficient of heat conduction and friction for dusty the flow of the boundary layer pressure gradient was studied Agranat (1988) (24). In addition to these studies for conduction of heat and diffusion for fluid that is cloudy along surface, many researchers considered dusty fluid flow along cylinder. Here we explained the Casson nano-fluid circulation over a stretching surface with temperature dispersion effect, and also flow rate in the absence of a source of heat. A huge proportion of experimentally obtained work is done in recent years to analyse the effect of heat production on forced convection heat transference. On the other hand this was explained by Tamoor et al. (25) the nature of Casson fluid under various stretching surfaces and boundary conditions been examined. Kumar et al. (Kumar, 2020) explain nanoparametric statistical models with linear coefficients and the spatial frequency soothing method to evaluate convection flow with 2nd slide now at stagnation point. This has a number of consequences experimenters to engage their brilliant minds in advancing exploration involving nano-fluids due to its indomitable demand in an extended variety of engineering and technology refined exercises. As a result, current researchers have focused on the temperature - dependent properties and applicability of nano particles by Mahanthesh et al. (Mahanthesh, 2020) he also explained Heat conduction improvement in nanoliquid flow across an extensible spinning disc due to nanoparticles, magnetic field, thermal, and exponential storage heat conduction elements. Researchers also evaluate our approach to those of earlier studies using a particular instance for the existing design. Another numerical study was carried out to investigate the mass and heat characteristics, as well as the impact of different velocity components. Recently work of Fazle and Stanford discoveries. then, using graphing, we gave a comparative summary of our talked about topic. Temporary stream with viscoelastic fluid in the condition of forced con-

vection heat and activation energy at the sheet will be investigated in future researches.

PROBLEM STATEMENT

Assume steady and in-compressible two-dimensional stagnation point stream of nanofluid along an extended sphere. Rectangular coordinate system (x^*,y^*) are adjusted in this manner a way that would be the sheets placed somewhere along x-axis fluid is confined in y > 0. To provide heat in the internal system, we have considered the convective boundary conditions with convective heat transfer coefficient h. Two rise to inverse there are influences connected so that the surface is aligned towards the x-axis extended protecting the beginning settled. We assist expect that the extended sheet warmth of convection stream (T_f) but also regular surrounding temperature (T_θ) with $T_f > T_\theta$. Throughout additional, we accept though that there is turbulence on the level liquid warmth T_f as well as a constant temperature T_∞. Sometimes $(T_f > T_\infty)$. Following above perceptions the oversee conditions of the stream are characterized as:

$$\frac{\partial u^*}{\partial x^*} + \frac{\partial v^*}{\partial y^*} = 0 \tag{1}$$

$$u^*\frac{\partial u^*}{\partial x^*} + v^*\frac{\partial u^*}{\partial y^*} + \frac{1}{\rho_f}\frac{\partial p^*}{\partial x^*} = (v)\left(1+\frac{1}{\beta}\right)\nabla^{*^2}u^* - \frac{\sigma B_{0u^*}^2}{\rho} \tag{2}$$

$$u^*\frac{\partial v^*}{\partial x^*} + v^*\frac{\partial v^*}{\partial y^*} + \frac{1}{\rho_f}\frac{\partial p^*}{\partial y^*} = (v)\left(1+\frac{1}{\beta}\right)\nabla^{*^2}v^* - \frac{\sigma B_0^2 v^*}{\rho} \tag{3}$$

$$u^*\frac{\partial T^*}{\partial x^*} + v^*\frac{\partial T^*}{\partial y^*} = \alpha^*\nabla^{*^2}T^* + \frac{(\rho c)_p}{(\rho c)_f}[D_B\nabla^*C^*.\Delta^*T^* + \frac{D_T}{T_\infty}\nabla^*T^*.\nabla^*T^*] \tag{4}$$

$$[u^*\frac{\partial C^*}{\partial x^*} + v^*\frac{\partial C^*}{\partial y^*}] = D_B\nabla^{*^2}C^* + (\frac{D_T}{T_\infty}\nabla^{*^2}T^* \tag{5}$$

Here we are considering,

- Velocity components as $u^*$and $v^*along\ the\ x-axis\ and\ y-axis\ respective$.
- ρ_f density of the fluid, ρ_p the mass density of nanoparticle, ν is the viscosity of kinematics, T stands for temperature, C_p is the structure of heat capacity, $\alpha^*$the warm diffusivity of most of the liquid.

Where boundary conditions for such fluids are

$u^* = cx^*$, $v^* = 0$, $-k\frac{\partial T^*}{\partial y^*} = h\left(T_f - T^*\right)$, $C^* = C_w$ at $y^* = 0$,

$D_B \frac{\partial C^*}{\partial y^*} + \frac{D_T}{T_\infty}\frac{\partial T^*}{\partial y^*} = 0, (for\ passive\ control)$

$C^* = C_W$, $(for\ active\ control)\ as\ y^* \to 0$

$u^* = ax^* + by^*$, $T^* = T_\infty$, $C^* = C_\infty\ as\ y^* \to \infty$ (6)

Here Positive constants with predictions of discourse time are a, b, and c.

K is the warm conductivity of the liquid, and h is the convective warmth move coefficient.

Using quasi constants

$x = x^*\sqrt{\frac{c}{\nu}}$, $y = y^*\sqrt{\frac{c}{\nu}}$, $u = \frac{1}{\sqrt{\nu c}}u^*$, $v = \frac{1}{\sqrt{\nu c}}v^*$, $p = \frac{1}{\mu c}p^*$,

$T = \frac{T^* - T_\infty}{T_f - T_\infty}$, $C = \frac{C^* - C_\infty}{C_w - C_\infty}$ (7)

The flow equation (1-5) take the following form, since $M = \sqrt{\frac{\sigma}{\rho}}\,\beta_0$

$$\frac{\partial u}{\partial x} + \frac{\partial v}{\partial y} = 0 \quad (8)$$

$$u\frac{\partial u}{\partial x} + v\frac{\partial u}{\partial y} + \frac{1}{\rho}\frac{\partial p}{\partial x} = \left(1 + \frac{1}{\beta}\right)\nabla^2 u - M^2 u \quad (9)$$

$$u\frac{\partial v}{\partial x} + v\frac{\partial v}{\partial y} + \frac{1}{\rho}\frac{\partial p}{\partial y}\left(1 + \frac{1}{\beta}\right)\nabla^2 v - M^2 v \quad (10)$$

$$pr[u\frac{\partial T}{\partial X} + v\frac{\partial T}{\partial y}] = \nabla^2 T + pr[N_b \nabla C.\nabla T + N_t \nabla T.\nabla T] \quad (11)$$

$$sc[u\frac{\partial C}{\partial X} + v\frac{\partial C}{\partial y}] = \nabla^2 C + \left(\frac{N_t}{N_b}\right)\nabla^2 T \quad (12)$$

The stream functions are defined as:

$u = \frac{\partial \psi}{\partial y}$, $v = -\frac{\partial \psi}{\partial x}$ (13)

Putting Equation (13) into Equations (8-12) and solved by eliminations of pressure $P_{xy} = P_{yx}$.

Following results are produced,

$(1 + \frac{1}{\beta})\nabla^4 \psi + \frac{\partial(\psi, \Delta^2 \psi)}{\partial(x,y)} - M^2 \nabla^2 \psi = 0$ (14)

$pr\left[\frac{\partial \psi}{\partial y}\frac{\partial T}{\partial x} - \frac{\partial \psi}{\partial x}\frac{\partial T}{\partial y}\right] = \nabla^2 T + pr\left[N_b \nabla C.\nabla T + N_t \nabla T.\nabla T\right]$ (15)

$sc\left[\frac{\partial\psi}{\partial y}\frac{\partial C}{\partial x}-\frac{\partial\psi}{\partial x}\frac{\partial C}{\partial y}\right]=\nabla^2 C+\left(\frac{N_t}{N_b}\right)\nabla^2 T$ (16)

The comparing limit conditions are

$\psi=0,\ \frac{\partial\psi}{\partial y}=x,\ \frac{\partial T}{\partial y}=-\frac{h}{k}\sqrt{\frac{v}{c}}(1-T),\ C=1\ at\ y=0,$

$\psi=\frac{a}{c}xy+\frac{1}{2}\gamma_1 y^2,\ T=0, C=0\ at\ y\to\infty$ (17)

Solution to equation (14-16) subject to the limit conditions (17) can be looked for as, subject to the limit conditions (5.17) can be looked for as,

$\psi(x,y)=xf(y)+g(y), T=\theta(y), C=\varnothing(y)$ (18)

Using equations (5.18) into equations (5.14-5.17) and we have ordinary differential equations as

$(1+\frac{1}{\beta})f'''+ff''-f'^2-M^2f'+C_1=0$, (19)

$(1+\frac{1}{\beta})g'''+fg''-f'g'-M^2g'+C_2=0$, (20)

$\theta''+pr[f\theta'+N_b\varnothing'\theta'+N_t\left(\theta'\right)^2]=0$ (21)

$\varnothing''+scf\varnothing'+\left(\frac{N_t}{N_b}\right)\theta''=0$ (22)

The relating limit conditions are as per the following

f(0)=0, $f'(0)=1$, f'$(\infty)=\frac{a}{c}$, $\theta'(0)=-\gamma(1-\theta(0))$, $\theta(\infty)=0$, g(0)=0, $g'(0)=0$, $g''(\infty)=\gamma_1, \varnothing(0)=1, \varnothing(\infty)=0$, (23)

$f', g', f'', g'', f''', g'''$ *shows* separation concerning 'y'. Here C_2, C_1 are unchanging element combination. β has been the (Past a porous) quasi component. *pr* is the count of Prandtl. N_t is basic variable of heat transfer rate, N_b is Molecular diffusion, γ is the variety of Biots while also Schmidt variety *sc* is described as:

$\beta=\mu_B\sqrt{\frac{2\pi c}{py}}$, $pr=\frac{v}{\alpha}$, $N_t=\frac{D_T}{T_\infty}\frac{(\rho c)_p}{(\rho c)_f}\frac{(T_f-T_\infty)}{v}$, $N_b=D_B\frac{(\rho c)_p}{(\rho c)_f}\frac{(\varnothing_w-\varnothing_\infty)}{v}$,

$\gamma=\frac{h}{k}\sqrt{\frac{\rho}{c}}$, $Sc=\frac{v}{D_B}$. (24)

Taking the breaking point y$\to\infty$ in Equation (19) a part from utilizing the limit situation $f'(\infty)=\frac{a}{c}$, we have $C_1=\frac{a^2}{c^2}$. An examination edges of the flow separation Eq. (19) infers f(y) uncovers that f(y)=$(\frac{a}{c}y)+A$ at y$\to\infty$.

Then equations (19) and (20) becomes:

$(1+\frac{1}{\beta})f'''+ff''-f'^2-M^2f'+\frac{a^2}{c^2}=0$, (25)

$(1+\frac{1}{\beta})g'''+fg''-f'g'-M^2g'-A\gamma_1=0$, (26)

$\theta''+pr[f\theta'+N_b\varnothing'\theta'+N_t\left(\theta'\right)^2]=0$, (27)

$\varnothing'' + scf\varnothing' + \left(\frac{N_t}{N_b}\right)\theta'' = 0$. (28)

From above equations we obtain when $\beta \to \infty$ for viscous fluid we obtain.

$g'(y) = \gamma_1 h(y)$. (29)

Using (29) into Eq. (26) now with restrictions in place of restriction $h(0) = 0$, $h'(\infty) = 1$ and we obtain

$(1+\frac{1}{\beta})h'' + fh' - f'h - M^2h - A = 0$ (30)

We also written in non-dimensional structure as, stream function ψ and skin friction τ_w that are here used in non-dimensional form is:

$\tau_w = \left(1+\frac{1}{\beta}\right)\left(\frac{\partial^2\psi}{\partial y^2} - \frac{\partial^2\psi}{\partial x^2}\right)$ (31)

Its dimensionless form is

$\tau_w = \left(1+\frac{1}{\beta}\right)\left[xf''(0) + \gamma_1 h'(0)\right]$ (32)

When τ_w=0 is given by

$x_s = \frac{-\gamma_1 h'(0)}{f''(0)}$- (33)

5.2 NUMERICAL SOLUTION

$f' = y_{1'} = y_2$

$f'' = y_{2'} = y_3$

$h = y_{3'} = y_4 = (\frac{\beta}{1+\beta})[-y_1y_3 + y_2^2 + M^2y_2 - \frac{a^2}{c^2}]$

$h' = y_{4'} = y_5$

$\theta = y_{5'} = y_6 = (\frac{\beta}{1+\beta})[-y_1y_5 + y_2y_4 + M^2y_4 + A]$

$\theta' = y_{6'} = y_7$

$\varnothing = y_{7'} = y_8 = -pr[y_1y_7 + N_by_9y_7 + N_t(y_{7)}^2]$

$\varnothing' = y_{8'} = y_9$

$\varnothing'' = y_{9'} = y_{10} = -scy_1y_9 - (\frac{N_t}{N_b})y_8$

Along with the boundary conditions:

$y_1(0) = 0$, $y_2(0) = 1$, $y_2(\infty) = \frac{a}{c}$,

$y_7(0) = -\gamma(1-\theta(0))$, $y_6(\infty) = 0$,

$y_8(0) = 1$, $y_8(\infty) = 0$,

$y_4(0) = 0$, $y_5(\infty) = 1$.

RESULT AND DISCUSSION

This segment illustrates the consequences of different attention of speed field and concentration fields. We have plotted the figures for different emerging parameter in

this unit. The main goal here is to examine the variety of real world boundaries that emerge from the Casson nano fluid model. To give an actual knowledge into the stream issue, was planned out for the speed region, sphere of warming, fixation and smoothes out. We define the continuity equation which is called equation (1) in this article, and then define equation (2-3) which is called momentum equation. Equation (4) shows temperature equation with nano-particles. The above boundary conditions shows that convective part (heat under the sheet) and in boundary conditions $y^* \to \infty$ shows that heat away from the sheet. To be able to elaborate a totally realistic embodied significance of either the flow issue, numerical results was mapped out in figures at the end individually for velocity field $(f'(0))$, distribution of temperature $(\theta(0))$ and concentration $(\varnothing(0))$ by stream lines. We have linear boundary condition. In Figure 5.2 we plotted the graph for the speed field, concentration and the streamlines. Fig 2 illustrated that how β affects the $h^{'}(y)$. Figure 2 represented the graph of velocity profile and taking with the different values of β. It demonstrates when a = 1, the incompressible downward motion h'(y) at a position falls as α = 1. which we really define the terms pr is Schmidt amount, Local Nusselt amount Sc Molecular diffusion N_b, thermophoresis boundary N_t and Number of Biots γ and warmth graph $\theta(y)$. Next in Figure 3 we draw a graph between $f'(y)$ and y-axis, for different values of β, taking the various values of alpha α. we observe that for something like a predetermined fee upsides β the warmth at a specific location decrease then it's a that would be increase with increase in β. In Figure 4 we plotted a graph of temperature profile $\theta(y)$ against α. We take different values of α and see that the temperature at a point decline with expanding β and it increment with expansion in α. Then we really generated a chart between the heat flux (y) and also the various upsides of pr in Figure 5. We found that the temperature at a point shrink as time has gone on expanding average Prandtl number pr. As a result, the depth of the temperature field decrease as growing Pr and as a result, increased constant heat flow at the interface. Figure 6 is plotted between the temperature profile $\theta(y)$ against the various values of β. We take different values of β and see so the warmth at a fixed site falls as the temperature rises α. Actual figures 7 and 8 we observe therefore, as the number of Schmidt expands Sc, Molecular diffusion N_b, Component of thermophoresis N_t, as well as Biot index γ the temperature gradient $\theta(y)$ also increase.

Tables (1-2) for such numerical values of the skin friction ratios are revealed, the heat in the area flow including the local independent amount of mass flow just for various particularly interested properties. Table of Contents of (1) It seems to be technically possible seen the fact that in our own calculated performance agree very well. Like Table (2) can be seen that amount the coefficient of skin friction $f''(0)$ falls as the number of individuals increases α while with increasing α, the tangentially related skin friction element $h'(0)$ continue to rise. In Table (2) whenever you check at it, it's certain that $\alpha < 1$, for fixed α, the magnitude of $f'(y)$ decreases as α increases β apparently. When $\alpha > 1$, however, $f'(y)$ grows with increasing α, which is consistent with the fact that the flow separation is now shrinking with raising α. The significance of the quasi Casson constant on skin frictions, global mass and heat flow on the radiative exponentially stretching sheet is addressed in Table (1). The goal of Table (2) is to study the impact of, N_t, N_b,Pr and Sc on the local warmth for anything like a quick fix upsidesα and b separately.

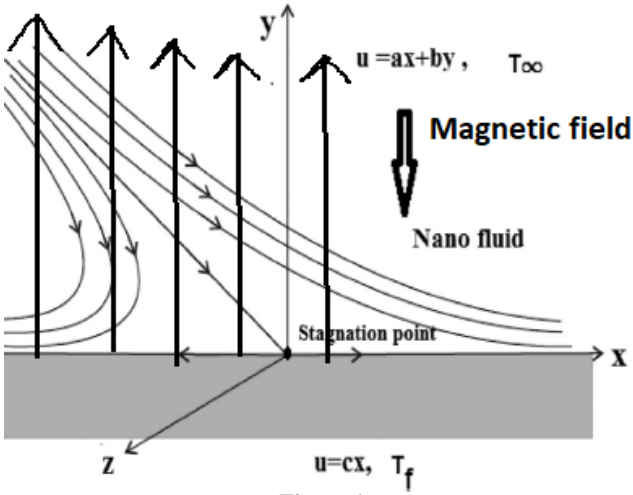

Figure 1
Physical description of the problem

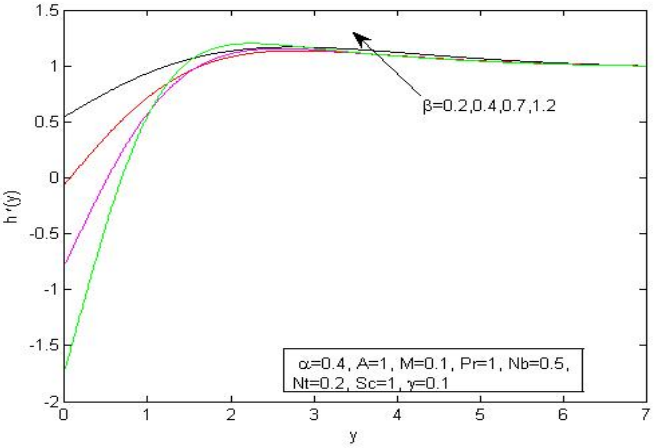

Figure 2: Consequence of β on $h'(y)$.

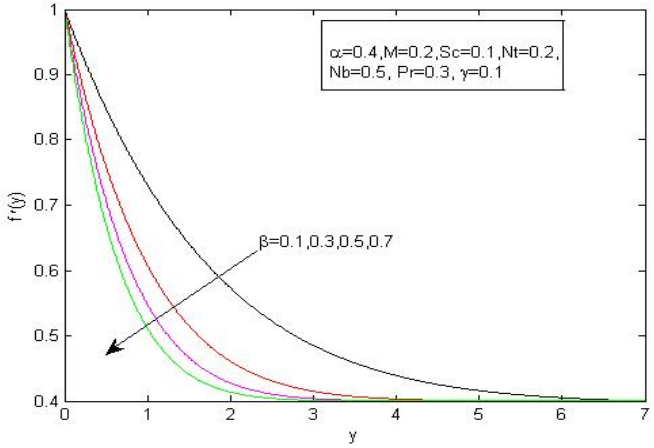

Figure 3: Consequence of β on $f'(y)$

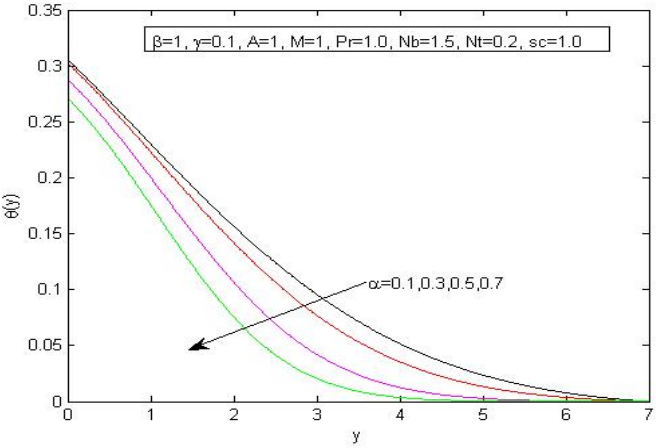

Figure 4: Consequences of α on $\theta(y)$.

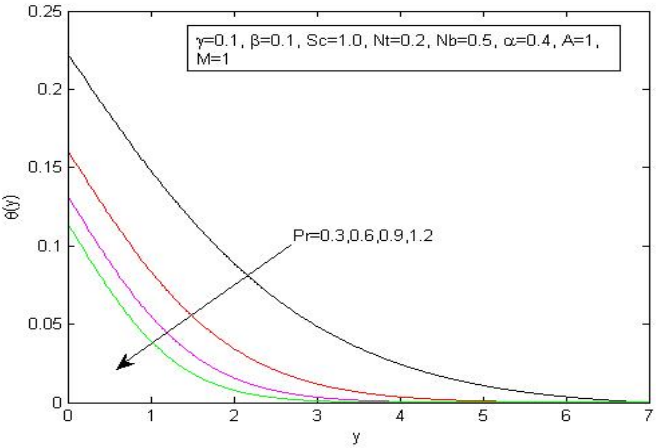

Figure 5: Consequence of pr on $\theta(y)$

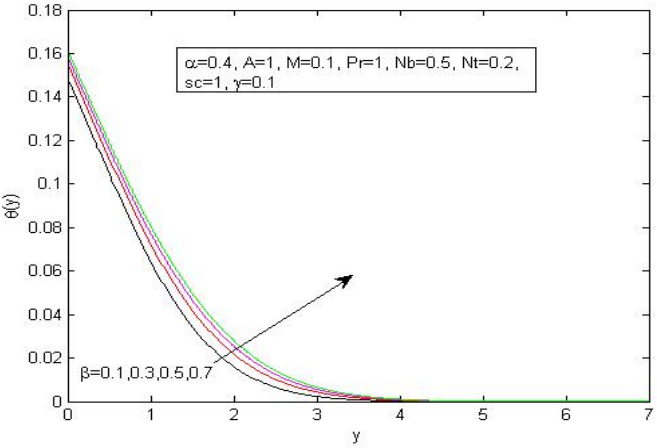

Figure 6: Consequences of β on $\theta(y)$.

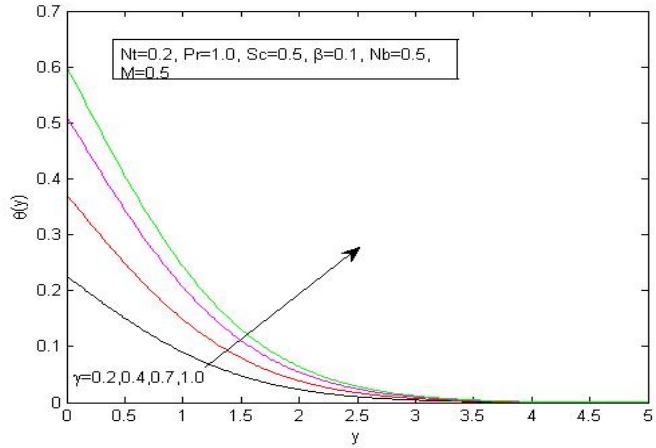

Figure 7: Consequences of γ on $\theta(y)$

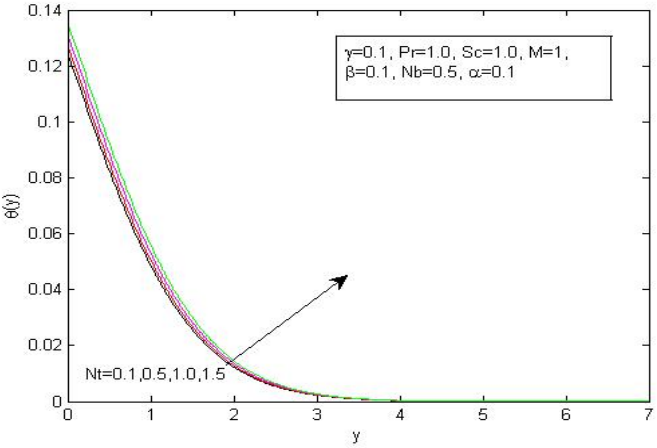

Figure 8: Consequences of Nt on $\theta(y)$.

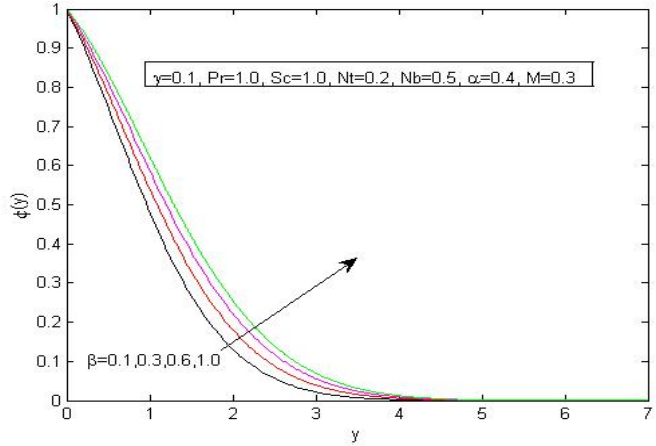

Figure 9: Consequences of β on $\phi(y)$

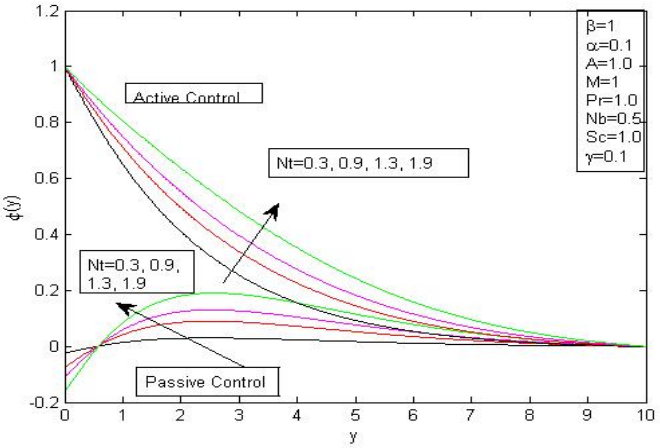

Figure 10: Consequences of Nt on $\phi(y)$

Table 1: Mathematical upsides of physical amounts when β, A, $-f''(0), h'(0), -\theta'(0), -\varphi'(0)$ for $N_t = 0.2, N_b = 0.5$, $Sc = 1.0 = Pr, \gamma = 0.5$, M=0.1.

β	M	A	$-f''(0)$	$h'(0)$	$-\theta'(0)$	*Active Control* $-\emptyset'(0)$
0.1	0.1	0.844536	-0.9807187	0.1548739	-0.431383	0.4975388
0.3	0.2	0.624733	-0.9106555	0.4881860	-0.452764	0.5344864
0.7	0.3	0.332823	-0.6725065	0.7791986	-0.497491	0.6047497
1	0.5	0.174311	-0.4243084	0.8964770	-0.530027	0.6528664
1.3	1.0	0.0044432	-0.1257159	0.9756863	-0.561204	0.6977471
1.5	1.2	-0.031612	0.09854497	1.0163065	-0.581230	0.7261481
1.9	1.3	-0.164264	0.33799786	0.1321389	-0.563880	0.6453479

Table 2: Mathematical upsides of physical amounts when $\gamma, A, -\theta'(0), and -\emptyset'(0), for\ N_t = 0.2, N_b = 0.5, Pr = 1, Sc = 1, M = 0.1, \alpha = 0.1, \beta = 5.0$

γ	M	N_t	N_b	Pr	Sc	$-\theta'(0)$	*Active Control* $-\emptyset'(0)$	*Passive Control* $-\emptyset'(0)$	$\theta'(0)$
0.1	0.3	0.2	0.5	1	1	-0.431383	-0.4975388	-0.581078	0.23243134
0.3	0.5					-0.431383	-0.4975388	-0.581078	0.23243134
0.5	0.1					-0.431383	-0.4975388	-0.581078	0.23243134
0.1	0.2	0.4	0.5	1	1	-0.405245	-0.4153802	-0.566146	0.45291754
		0.6				-0.380927	-0.3477223	-0.551356	0.66162769
0.1	0.1	0.2	0.1	1	1	-0.533225	-0.0689986	-0.581078	1.16215672
			0.3			-0.480387	-0.4043269	-0.581078	0.38738557
			0.5			-0.431383	-0.4975388	-0.581078	0.23243134
0.1	0.3	0.2	0.5	2	1	-0.555895	-0.4640803	-0.894596	0.35783866
				2.5		–0.58979	-0.4556473	-1.022521	0.40900840
0.1	0.5	0.2	0.5	1	2	-0.398839	-0.8528104	-0.574385	0.22975431
					2	-0.390184	-0.9944334	-0.572156	0.22886256

Table 3: Mathematical upsides of physical amount when r, N_t, N_b, Pr, Sc and M for $r_1 = 1$

						Shooting		bvp4c	
R	N_t	N_b	Pr	Sc	M	$-\theta'(0)$	—	$-\theta'(0)$	$\varphi'(0)$
						$\varphi'(0)$			
0.1	0.2	0.5	1	1	0.5	0.08152		0.08152	0.55954
						0.55954			
0.3						0.17753		0.17753	0.54870
						0.43578			
0.5						0.23158		0.23158	0.53694
						0.76558			
0.1	0.4	o.5	1	1	0.5	0.08134		0.08115	0.47016
						0.54676			
	0.6					0.08115		0.08563	0.54456
						0.53168			
0.1	0.2	0.1	1	1	0.5	0.08563		0.08657	0.55739
						0.54016			
		0.3				0.08678		0.08139	0.88630
						0.47789			
		0.5				0.08044		0.08044	1.01974
						0.52168			
0.1	0.2	0.5	2	1	0.5	0.08013		0.07757	0.43876
						0.54495			
			2.5			0.04631		0.08040	0.55687
						0.55865			
0.1	0.2	0.5	1	2		0.08309		0.08563	0.05445
						0.88630			
				2.5		0.08152		0.07669	0.06777
						1.01978			
0.1	0.2	0.5	1	1	1	0.08234		0.06756	0.07878
						0.51915			
					2	0.08567		0.08117	0.05545
						0.52244			

5.4 CONCLUDING REMARKS

In present examination, the calculated stagnation point along with nanofluid stream for the warm while also masses trades more than that straightforwardly expanding out chart is watched out for, we examined the inspected the viscoelastic nano liquid's two-dimensional stagnation - point flow stream with convection limit condition. A productive insightful technique of shooting method is used to determine the system of governance of functions' error terms. Also graphs and tables are now used to study the flow controlling properties which is obtained by using MATLAB.

- Variation in the stretching parameters does not affect the location of the stagnation point
- Angle of incidence decreases, while increasing the stretching parameter in the normal direction.
- Biot number and Schmidt numbers increase with an increase in the kinematic viscosity of the base fluid.
- Prandtl identification, Biots number decrease with an increase in Brownian motion.

2. Author's Contributions

All author's contributed equally to the writing of this paper. All author's read and approved the final manuscript.

References

[1] A. Y. Ghaly, & E. M. Elbarbary, Radiation effect on MHD free-convection flow of a gas at a stretching surface with a uniform free stream. Journal of Applied Mathematics, 2(2)(2002), 93-103.

[2] H. M. H. Masuda, & M. S. M. Satoh, (1996). Fabrication of gold nanodot array using anodic porous alumina as an evaporation mask. Japanese Journal of Applied Physics, 35(1B), L126.

[3] S. U. S. Choi, Enhancing thermal conductivity of fluids with nanoparticles, in: D.A. Siginer, H.P. Wang (Eds.), Developments and Applications of Non- Newtonian Flows, vol. 66ASME, New York, 1995, p.99.

[4] T. R. Mahapatra, A. S. Gupta, Heat transfer in stagnation point flow towards a stretching sheet, Heat Mass Transfer 38 (2002) 521.

[5] A. Aziz, A similarity solution for laminar thermal boundary layer over a flat plate with convective surface boundary condition, Commun. Nonlinear Sci. Numer. Simulat. 14 (2009) 1068.

[6] K. Hiemenz, Die Grenzschicht an einem in den gleichförmigen Flüessigkeitsstrom eingetauchten geraden Kreiszylinder, Dinglers Polytech. J. (1911) 321.

[7] L. Howarth, On the calculation of steady flow in the boundary layer near the surface of a cylinder in a stream. AERONAUTICAL RESEARCH COUNCIL LONDON (UNITED KINGDOM)(1934).

[8] F. Homann, Einfluß großer zähigkeit bei strömung um zylinder. Forschung auf dem Gebiet des Ingenieurwesens A, 7 (1936), 1-10.

[9] A. Bilal, N. Jahan, A. Ahmed, S. N. Bilal,S. Habib, & S. Hajra, Phytochemical and pharmacological studies on Ocimum basilicum Linn-A review. International Journal of Current Research and Review, 4(23)(2012), 73-83.

[10] A. Aziz, Hydrodynamic and thermal slip flow boundary layers over a flat plate with constant heat flux boundary condition, Commun. Nonlinear Sci. Numer. Simulat. 15 (2010) 580.

[11] J. Buongiorno, Convective transport in nano fluids, ASME J. Heat transfer 128 (2006) 240.

[12] R. Ellahi, Arshad Riaz, Analytical solutions for MHD flow in a third-grade fluid with variable viscosity, Math. Comput. Model. 52 (2010) 1783.

[13] R. Ellahi, Effects of the slip boundary condition on non-Newtonian flows in a channel, Commun. Nonlinear Sci. Numer. Simulat. 14 (2009) 1377.

[14] R. Ellahi, S. Afzal, Effects of variable viscosity in a third grade fluid with porous medium: an analytic solution, Commun. Nonlinear Sci. Numer. Simulat. 14 (2009) 2056.

[15] Y. Y. Lok, N. Amin & I. Pop, Unsteady mixed convection flow of a micropolar fluid near the stagnation point on a vertical surface. International journal of thermal sciences, 45(12)(2006), 1149-1157

[16] L. J. Crane, Flow past a stretching plate. Zeitschrift für angewandte Mathematik und Physik ZAMP, 21(1970), 645-647.

[17] D. R. Mahapatra, & S. Gopalakrishnan, A spectral finite element model for analysis of axial–flexural–shear coupled wave propagation in laminated composite beams. Composite Structures, 59(1) (2003), 67-88.

[18] P. R. Sharma & G. Singh (2009). Effects of variable thermal conductivity and heat source/sink on MHD flow near a stagnation point on a linearly stretching sheet, Journal of Applied Fluid Mechanics, 2(1) 2009,13-21.

[19] F. Labropulua, I. Pop, Non-orthogonal stagnation-point flow towards a stretching surface in a non-Newtonian fluid with heat transfer, Int. J. Therm. Sci. 49 (2010) 1042.

[20] S. Nadeem, R. Mehmood, N. S. Akbar, Nanoparticle analysis for non-orthogonal stagnation point flow of a third order fluid towards a stretching surface, J. Comput. Theor. Nanosci. 10 (2013) 2737-2747.

[21] A. Ishak, K. Jafarb, R. Nazar, I. Pop, MHD stagnation point flow towards a stretching sheet, Physica A 388 (2009) 3383.

[22] A. Ishak, Similarity solutions for flow and heat transfer over a permeable surface with convective boundary condition, Appl. Math. Comput. 217 (2010) 842.

[23] A. Ghaffari, T. Javed & F. Labropulu, Oblique stagnation point flow of a non-Newtonian nanofluid over stretching surface with radiation: a numerical study. Thermal Science, 21(5)(2017), 2139-2153.

[24] V. M. Agranat, Effect of pressure gradient of friction and heat transfer in a dusty boundary layer. Fluid Dynamics, 23(5) (1988), 729-732.

[25] M. Tamoor, M. Waqas, M. I. Khan, A. Alsaedi & T. Hayat, Magnetohydrodynamic flow of Casson fluid over a stretching cylinder. Results in physics, 7(2017), 498-502.